

1 **Age-dependent changes in transcription factor FOXO targeting in *Drosophila melanogaster***

2 Allison Birnbaum^{1#}, Xiaofen Wu^{2,3#}, Marc Tatar⁴, Nan Liu^{2*}, Hua Bai^{1*}

3

4 1 Department of Genetics, Development, and Cell Biology, Iowa State University, Ames, IA

5 50011, USA

6 2 Interdisciplinary Research Center on Biology and Chemistry, Chinese Academy of Sciences,

7 Shanghai, 201210, China

8 3 University of Chinese Academy of Sciences, Beijing, 100049, China

9 4 Department of Ecology and Evolutionary Biology, Brown University, Providence, RI, 02912,

10 USA

11

12 **Email:**

13 Allison Birnbaum: abirbba1@iastate.edu

14 Xiaofen Wu: xiaofenwu@sioc.ac.cn

15 Marc Tatar: Marc_Tatar@brown.edu

16 Nan Liu: liunan@sioc.ac.cn

17 Hua Bai: hbai@iastate.edu

18

19 *** Corresponding Authors:**

20 Nan Liu

21 Hua Bai

22

23 **# Equal contribution**

39 **Summary**

40 FOXO transcription factors have long been associated with longevity control and tissue
41 homeostasis. Although the transcriptional regulation of FOXO have been previously
42 characterized (especially in long-lived insulin mutants and under stress conditions), how normal
43 aging impacts the transcriptional activity of FOXO is poorly understood. Here, we conducted a
44 chromatin immunoprecipitation sequencing (ChIP-Seq) analysis in both young and old wild-type
45 fruit flies, *Drosophila melanogaster*, to evaluate the dynamics of FOXO gene targeting during
46 aging. Intriguingly, the number of FOXO-bound genes dramatically decreases with age (from
47 2617 to 224). Consistent to the reduction of FOXO binding activity, many genes targeted by
48 FOXO in young flies are transcriptionally altered with age, either up-regulated (FOXO-
49 repressing genes) or down-regulated (FOXO-activating genes). In addition, we show that many
50 FOXO-bound genes in wild-type flies are unique from those in insulin receptor substrate *chico*
51 mutants. Distinct from *chico* mutants, FOXO targets specific cellular processes (e.g., actin
52 cytoskeleton) and signaling pathways (e.g., Hippo, MAPK) in young wild-type flies. FOXO
53 targeting on these pathways decreases with age. Interestingly, FOXO targets in old flies are
54 enriched in cellular processes like chromatin organization and nucleosome assembly.
55 Furthermore, FOXO binding to core histone genes is well maintained at aged flies. Together, our
56 findings provide new insights into dynamic FOXO targeting under normal aging and highlight
57 the diverse and understudied regulatory mechanisms for FOXO transcriptional activity.

58 **Keywords:** Forkhead transcription factor FOXO, ChIP-Seq, Transcriptional regulation,
59 Longevity control, Insulin, Hippo, MAPK, Histone

60

61

62 **Introduction**

63 The process of aging is accompanied by a decline in physiological function and cellular
64 maintenance. It is known that aging dramatically alters gene expression and transcription factor
65 activity (Lopez-Otin, Blasco, Partridge, Serrano, & Kroemer, 2013). The protein family of
66 Forkhead Box subfamily O transcription factors, or FOXO, has been shown to play an important
67 role in growth, development, stress resistance, and longevity (Greer & Brunet, 2005). FOXO
68 functions downstream of insulin/insulin-like growth factor (insulin/IGF) signaling and is
69 negatively regulated by PI3K-Akt pathway (Brunet et al., 1999). FOXO transcriptionally
70 regulates numerous target genes involving metabolism, cell cycle progression, stress, and
71 apoptosis (Kitamura et al., 2002; Kops et al., 2002; Martins, Lithgow, & Link, 2016; Medema,
72 Kops, Bos, & Burgering, 2000). Additionally, FOXO proteins were first implemented in lifespan
73 extension in *Caenorhabditis elegans* where insulin-like receptor mutant *daf-2* extends lifespan
74 via FOXO homolog *daf-16* (Kenyon, Chang, Gensch, Rudner, & Tabtiang, 1993). This lifespan
75 extension through insulin/IGF signaling has been observed across species, from worm to fly to
76 mammal (Holzenberger et al., 2003; Kenyon et al., 1993; Tatar et al., 2001). Studies have found
77 that lifespan extension effects of insulin/IGF deficiency depend on FOXO activity, probably
78 through the transcriptional regulation of key longevity assurance pathways such as xenobiotic
79 resistance (Slack, Giannakou, Foley, Goss, & Partridge, 2011; Yamamoto & Tatar, 2011).
80 However, how FOXO elicits this response remains to be fully elucidated.

81 FOXO activity is not solely dependent on insulin/IGF signaling. FOXO proteins undergo
82 posttranslational modifications in response to other cellular stress signals. Oxidative stress
83 promotes Jun-N-terminal Kinase (JNK)-dependent phosphorylation of mammalian FOXO4 and
84 its nuclear translocation. FOXO proteins can also be activated and phosphorylated by

85 mammalian Sterile 20-like kinase 1 (MST1), to extend lifespan (Dansen & Burgering, 2008;
86 Essers et al., 2004; Lehtinen et al., 2006). In response to DNA damage, cyclin-dependent kinase
87 2 (CDK2) can phosphorylate and regulate mammalian FOXO1 to delay cell cycle progression
88 and induce apoptosis (Huang & Tindall, 2006). FOXO proteins are also involved in tumor
89 suppression activity and responds to oncogenic stress (Dansen & Burgering, 2008). Interestingly,
90 two recent chromatin immunoprecipitation-sequencing (ChIP-Seq) studies revealed that FOXO
91 proteins are enriched at the promoters of many target genes in well-fed wild-type *C. elegans* and
92 *Drosophila* (Alic et al., 2011; Riedel et al., 2013).

93 Although insulin/IGF signaling is well-known aging regulators, how insulin/IGF
94 signaling is altered during normal aging remains largely unclear. It is generally believed that
95 insulin/IGF signaling declines with age. This is primarily based on age-dependent decrease in the
96 expression of FOXO target genes (Demontis & Perrimon, 2010; Rera, Clark, & Walker, 2012).
97 However, it remains to be determined how aging impacts FOXO transcriptional activity and
98 DNA binding capacity of FOXO transcription factors. Here, we conducted a ChIP-Seq analysis
99 to investigate FOXO binding dynamics under normal aging in *Drosophila*. Intriguingly, we
100 found that the number of FOXO-bound regions sharply decrease with age. The age-related
101 decrease in FOXO binding is correlated with either the transcriptional activation of FOXO-
102 repressing genes, or the downregulation of FOXO-activating genes during normal aging.
103 Furthermore, we observed strong FOXO nuclear localization in well-fed wild-type flies, while
104 FOXO targets distinct sets of genes between wild-type and insulin mutants. Taken together, our
105 findings provide new evidence linking age-dependent FOXO transcriptional activity to its role in
106 longevity control and tissue maintenance.

107

108 **Results**

109 **FOXO exhibits constitutive nuclear localization in young and old adult fat body**

110 To examine whether *Drosophila* FOXO activity changes with aging, we first performed
111 immunofluorescent staining using a polyclonal antibody against *Drosophila* FOXO to monitor
112 the FOXO nuclear localization in wild-type flies (yw^R) at two different ages, two-week-old
113 (young flies) and five-week-old (aged flies). Intriguingly, FOXO proteins exhibited constitutive
114 nuclear localization in abdominal fat body tissue of well-fed wild-type female flies (yw^R), where
115 insulin/IGF signaling is presumably active (Figure 1A). The constitutive nuclear localization of
116 FOXO was also found in another wild-type line, *Oregon R* (*OreR*) (Figure S1). FOXO proteins
117 remained nuclear localization during aging, while the colocalization of FOXO with nuclear
118 DAPI staining slightly declined in aged fat body tissue (Figure 1A-1B). Compared to adult fat
119 body, indirect flight muscles from both two-week-old and five-week-old female flies showed
120 low FOXO nuclear localization (Figure 1C, 1D, S1). Thus, these results suggest that FOXO
121 could be activated in well-fed wild-type flies to regulate the expression of its target genes, which
122 is consistent with recent ChIP-Seq studies (Alic et al., 2011; Riedel et al., 2013).

123 **ChIP-Seq analysis reveals age-dependent reduction of FOXO-targeted DNA binding**

124 To further investigate the FOXO transcriptional activity under normal aging, we
125 performed ChIP-Seq analysis on young (2-week) and aged (5-week) female wild-type flies.
126 Using Illumina high-throughput sequencing, we obtained a total of 261 million reads from
127 FOXO ChIP and input DNA samples at two ages. On average, 90.08% of unique reads were
128 mapped to annotated *Drosophila* reference genome (Figure S2A, Table S1:List 24). Intriguingly,
129 our ChIP-Seq analysis revealed that the number of FOXO-bound genomic regions (based on
130 MACS2 peak calling) dramatically decreased with age (Figure 2A). There were 9273 peaks

131 identified in young flies (corresponding to 2617 protein coding genes), whereas in aged flies
132 only 1220 peaks (224 genes) were detected (Figure 2A, Table S1:List 5-8). About 170 genes
133 were shared between two ages. For most of the peaks, a reduction in peak size or a disappearance
134 of peaks was observed in aged flies (Figure 2B), while the FOXO binding to a few genomic
135 regions remained unchanged during aging (Figure 2C). The reduction of FOXO-bound regions
136 was not due to the decreased quantity of immunoprecipitated genomic DNA (data not shown). In
137 fact, equal amount of ChIP and input DNA samples were used to generate Illumina sequencing
138 libraries. In addition, a correlation matrix plot showed that the reads from 2-week-old FOXO
139 ChIP samples were most divergent from the input and 5-week-old ChIP samples, further
140 suggesting the differential FOXO-DNA binding activity between young and aged flies (Figure
141 S2B).

142 Pathway analysis revealed that FOXO target genes at young ages were enriched in
143 pathways like Hippo, Wnt, TGF-beta, MAPK, and insulin resistance pathways (Figure 2D, Table
144 S1:List 10). FOXO was also targeting genes involved in nervous system development, motor
145 neuron stabilization, and regulation of synaptic tissue communication (Table S1:List 10).
146 Additionally, we found that FOXO bound to the genomic regions containing key autophagy
147 regulators (*Atg3*, *Atg17*, *Tor*, *wdb*, *Pten*), which is consistent to previous known functions of
148 FOXO in autophagy and tissue homeostasis (Demontis & Perrimon, 2010). Many Rho and small
149 GTPase proteins, as well as actin cytoskeleton pathways, are also targeted by FOXO at young
150 ages. Many of these FOXO-targeted pathways were absent in aged flies. Instead, processes like
151 nucleosome assembly and chromatin organization were enriched as FOXO-bound targets in aged
152 flies (Figure 2D, Table S1:List 11). Interestingly, strong FOXO binding was maintained at many
153 core histone genes at old ages (Figure 2C, 2E).

154 The age-dependent changes in FOXO binding activity were verified by quantitative PCR
155 (ChIP-qPCR). The FOXO binding to the promoters of two known target genes, insulin receptor
156 *InR* and adipose triglyceride lipase *bmm*, were first tested in ChIP-qPCR analysis (Figure 2E).
157 FOXO showed similar binding enrichment (6~7 fold) at *InR* locus between young and old ages
158 (Figure 2E). On the other hand, the FOXO binding to *bmm* promoter slightly decreased with age
159 (Figure 2E). We also confirmed that FOXO binding remained unchanged at two histone loci
160 (*his1:CG33804* and *his2B:CG33908*), while the FOXO enrichment at two newly identified target
161 genes, *jim* (C2H2 zinc finger transcription factor) and *dlg1* (a key factor for the formation of
162 septate junctions and synaptic junctions), decreased dramatically at old ages (from 80~90-fold to
163 3~8-fold) (Figure 2E). Thus, our ChIP-qPCR analysis confirmed that FOXO binding activity was
164 altered in many target loci during normal aging.

165 **FOXO-bound genes show age-dependent transcriptional changes**

166 We next examined whether age-dependent changes in FOXO binding is correlated to age-
167 regulated transcription of FOXO target genes. To do so, we first compared our FOXO ChIP-Seq
168 results to previously published aging transcriptomic analysis on aging *Drosophila* tissues, such
169 as fat body and head tissue. Out of 2447 FOXO target genes (uniquely bound by FOXO at young
170 ages), 408 of them were differentially expressed in aging fat body (172 downregulated, 236
171 upregulated) (Figure 3A, Table S1:List 12), while 845 target genes were differentially expressed
172 in aging head tissue (626 downregulated, 219 upregulated) (Figure 3C, Table S1:List 13).
173 Interestingly, a majority of the FOXO-bound genes showed no age-related transcriptional
174 changes, which is similar to previous studies showing the FOXO binding at the promoters of
175 large number of so-called poised genes (Webb, Kundaje, & Brunet, 2016; Webb et al., 2013).
176 Gene ontology analysis revealed that FOXO target genes differentially expressed in aging fat

177 body were enriched for processes and signaling pathways like chromatin organization, histone
178 modification, hippo signaling, peroxisome, and hormone biosynthesis (Figure 3B, Table
179 S1:List14). On the other hand, the differentially expressed FOXO targets in aging head tissue
180 were enriched for pathways and processes involving Wnt, Hippo, G protein-couple receptor
181 (GPCR), axon guidance, synapse organization, and actin cytoskeleton (Figure 3D, Table
182 S1:List15).

183 Although many FOXO-bound target genes exhibited differential expression during aging,
184 it remains unclear whether decreased FOXO-binding activity at old ages contributes to age-
185 dependent transcriptional changes of these FOXO target genes. To further determine the
186 relationship between FOXO binding and transcriptional changes of FOXO target genes, we
187 performed a RNA-Seq analysis using head tissues dissected from wild-type flies and a *foxo* null
188 mutants (*foxo*^{c431}), a site-specific deletion mutant generated by CRISPR/Cas9 (Figure 4A-4B).
189 Out of 2617 FOXO-bound target genes, 101 of them were upregulated in *foxo*^{c431} mutants, while
190 300 were downregulated in the mutants (Figure 4C, Table S1:List 16), suggesting that FOXO
191 binding might be important to repress or activate at least a subset of target genes. Based on these
192 data, FOXO target genes can be sorted into three classes, FOXO-repressing (101 genes), FOXO-
193 activating (300 genes), and FOXO-no regulation (1621 genes).

194 We next asked how reduced FOXO binding during aging impacts the expression of
195 FOXO target genes. To do this, we first constructed new transcriptomic profiles from wild-type
196 head tissue at four different ages, 3d, 15d, 30d, and 45d (Table S1:List 17). Interestingly, among
197 three classes of FOXO target genes, FOXO-repressing genes exhibited an increased expression
198 in old flies, whereas FOXO-activating genes were progressively downregulated with age.
199 Expression of FOXO-no regulation genes, on the other hand, did not significantly change during

200 aging (Figure 4D). Taken together, these results suggest that age-associated decrease in FOXO
201 binding might contribute directly to the transcriptional alterations of FOXO target genes in old
202 flies.

203 **FOXO binding differs between wild-type and insulin/IGF mutants**

204 FOXO binding activity has been primarily studied by evaluating its response to IIS
205 signaling (Alic et al., 2011; Bai, Kang, Hernandez, & Tatar, 2013; Murphy, 2006; Riedel et al.,
206 2013; Webb et al., 2016). However, our observations on FOXO nuclear localization and DNA
207 binding in well-fed wild-type flies suggest that there might be distinct FOXO transcriptional
208 activity independent of insulin/IGF signaling. To test this possibility, we compared FOXO ChIP-
209 Seq datasets from the present study (young wild-type) and our previous analysis on insulin
210 receptor substrate *chico* mutants (Bai et al., 2013). Intriguingly, large number of FOXO-bound
211 genes were not shared between wild-type and *chico* mutants. There were 1992 FOXO target
212 genes unique to wild-type, while 1393 genes unique to *chico* mutants (Figure 5A, Table S1:List
213 18). Furthermore, distinct FOXO targets between wild-type and *chico* mutants were
214 differentially expressed with age (Figure 5B). About 844 age-regulated genes were only bound
215 by FOXO in wild-type flies, while 577 genes unique to *chico* mutants (Table S1:List 19). We
216 found that age-regulated FOXO targets unique to *chico* mutants were enriched in metabolic
217 pathway and oxidative-reduction, while those unique to wild-type flies were enriched for
218 chromatin organization, axon guidance, Hippo and MAPK signaling pathways (Figure 5C, Table
219 S1:List 20-21). When examining each pathway in detail, we noticed that FOXO targets in Hippo
220 and MAPK/EGFR signaling pathways were found in both wild-type and *chico* mutants, although
221 different target genes were apparent between the two conditions (Figure S3-S4).

222 To test if distinct FOXO binding activity observed between wild-type flies and
223 insulin/IGF mutants is conserved across species, we reanalyzed the recent *C. elegans* *Daf-16*
224 ChIP-seq study (Riedel et al., 2013). Interestingly, wild-type worms also showed different *Daf-*
225 *16* binding activity from *daf-2* mutants. There were 2296 genes uniquely bound by *Daf-16* to
226 wild-type worms, while 996 were unique to *daf-2* mutants (Figure 5D, Table S1:List 22). Gene
227 ontology analysis showed that FOXO transcription factors targeted similar pathways in wild-type
228 flies and worms. These pathways were MAPK signaling, cell cycle, FOXO signaling, nervous
229 system development, chromatin remodeling, mTOR signaling, autophagy, and oxidative stress
230 (Figure 5E, Table S1:List 23). Thus, insulin/IGF-independent FOXO transcriptional activity may
231 be an evolutionarily conserved cellular mechanism.

232 **Enriched FOXO motifs in wild-type flies**

233 A signature of FOXO targeting is the 8-nucleotide long canonical binding motif, 5'-
234 TTGTTTAC-3', which is conserved across species (Bai et al., 2013; Furuyama, Nakazawa,
235 Nakano, & Mori, 2000; Webb et al., 2013). This motif is typically found upstream of the gene
236 coding site in the enhancer or promoter region (Eijkelenboom, Mokry, Smits, Nieuwenhuis, &
237 Burgering, 2013; Webb et al., 2013). To search for FOXO consensus sequence in the FOXO-
238 bound genomic regions found in young wild-type flies, we conducted motif analysis using the
239 Homer motif finding tool. We used peaks with at least a 2-fold enrichment that were less than
240 2000 bp in length, and we searched for motifs within 200 bp surrounding the peak region. When
241 insect motif databases were used, we identified only one known motif for Trl ($p < 10^{-70}$), a
242 GAGA-factor that also found in previous ChIP-Seq data from *C. elegans* (Riedel et al., 2013)
243 (Table 1). When searching against known mammalian motifs, a motif for FOXO1 (with
244 canonical consensus, TGTTTAC) was detected with low significance ($p < 10^{-4}$). (Table 1). Next,

245 using *de novo* motif search we found that FOXO-bound regions were enriched with motifs for
246 transcription factors hb, Adf1, and Aef1. Lastly, we performed Homer *de novo* motif search and
247 identified a motif for RAP1, a *Saccharomyces cerevisiae* gene that is part of the Myb/SAINT
248 domain family, which was also found in a previous *Drosophila* FOXO ChIP-on-ChIP study (Alic
249 et al., 2011). Together, these findings suggest that in wild-type flies FOXO may recognize a
250 unique set of motifs that is different from the canonical consensus sequence.

251

252 **Discussion**

253 As a key player in longevity control, FOXO transcription factors and their direct targets
254 have been well characterized in many model systems (Alic et al., 2011; Bai et al., 2013; Riedel et
255 al., 2013; Webb et al., 2013). However, whether and how FOXO transcriptional activity changes
256 with age is unclear. In the present study, we performed a ChIP-Seq analysis to examine the
257 FOXO binding activity during *Drosophila* aging. Intriguingly, genome-wide FOXO-binding
258 underwent an immense reduction at old ages. Consistently, genes that are negatively regulated by
259 FOXO showed an increased expression with age, whereas the FOXO-activating genes were
260 downregulated in aged flies. Thus, age-associated decrease in FOXO binding is tightly linked to
261 the transcriptional alterations of FOXO target genes at old ages. In addition, we found that
262 FOXO targets distinct sets of genes between wild-type and insulin/IGF mutants across species,
263 suggesting a conserved insulin/IGF-independent transcriptional regulation by FOXO
264 transcription factors.

265 Changes in transcription factor binding patterns at different stages of life are not
266 exclusive to FOXO. In *C. elegans*, FoxA/PHA-4 exhibits differential binding patterns at different
267 stages of development to regulate organogenesis (Zhong et al., 2010). Similar to FOXO binding

268 pattern, PHA-4 also exhibited binding at poised locations in the genome. The loss of specific
269 FOXO targeting with age observed in the present study could be caused by either altered post-
270 translational modification of FOXO, or changes in co-transcriptional regulation between FOXO
271 and its partners. It is known that FOXO co-factors play an important role in fine-tuning FOXO
272 transcriptional activity (Alic et al., 2011; Essers et al., 2004; Riedel et al., 2013; Webb et al.,
273 2016). These co-factors include post-translational modifiers and nuclear interacting partners
274 which aid FOXO in recruitment to target binding sites (Daitoku, Sakamaki, & Fukamizu, 2011;
275 van der Vos & Coffey, 2008). A previous meta-analysis identified the binding motifs of many of
276 novel transcription factors (EST, NRF and GATA factors) are enriched at FOXO target genes
277 with age-related expression patterns (Webb et al., 2016), which suggests that the interplay
278 between FOXO and these transcription factors may contribute to the altered FOXO
279 transcriptional activity during normal aging. Certain mammalian FOXO co-factors, such as
280 peroxisome proliferator-activated receptor gamma (PPAR γ), and its coactivator (PGC-1 α)
281 interact with FOXO and compete for binding with FOXO and β -Catenin (Olmos et al., 2009;
282 Polvani, Tarocchi, & Galli, 2012). FOXO acts as a repressor of PPAR γ gene transcription, and
283 this repression is lost later in life, suggesting a reduction of FOXO binding at PPAR γ locus
284 (Armoni et al., 2006; Polvani et al., 2012). Besides PPAR γ and PGC-1 α , many other
285 transcription co-regulators and post-translational modifiers have been shown to be involved in
286 transcriptional co-regulation of FOXO target genes, which may play important roles in
287 modulating FOXO transcriptional activity during aging (Daitoku et al., 2011; van der Horst &
288 Burgering, 2007).

289 Many FOXO-targeted cellular processes (e.g., nervous system development and actin
290 cytoskeleton) and signaling pathways (e.g., Hippo, Wnt, TGF-beta, MAPK) are uniquely

291 enriched in young wild-type, but not in *chico* mutants. Majority of these FOXO targets show
292 age-dependent differential expression patterns. The Hippo pathway was initially characterized
293 for its role in controlling organ size during development, but recently it has been shown to
294 involve in autophagy, oxidative stress response, and aging (Lehtinen et al., 2006; Mao, Gao, Bai,
295 & Yuan, 2015; Udan, Kango-Singh, Nolo, Tao, & Halder, 2003). In adult mice, suppression of
296 Hippo signaling improved cell proliferation and heart tissue regeneration and is a regulator of
297 tissue homeostasis (Heallen et al., 2013). Thus, Hippo signaling may be one of the major FOXO
298 targets in the regulation of cellular homeostatic and longevity. MAPK signaling is involved in
299 tissue homeostasis with aging (Jiang, Grenley, Bravo, Blumhagen, & Edgar, 2011; Lee & Sun,
300 2015), and is also enriched among FOXO-bound target genes in wild-type flies. Both the EGFR
301 and JNK cascades of the MAPK signaling pathway are targeted by FOXO. The target genes
302 involved in the EGFR signaling exhibit transcriptional alterations with age in the wild-type fly.
303 In adult *Drosophila*, EGFR signaling is responsible for maintaining midgut epithelial
304 homeostasis in the adult and has also been shown to regulate cytoskeletal modulation and
305 autophagy (Hazan & Norton, 1998; Jiang et al., 2011; Tan, Lambert, Rapraeger, & Anderson,
306 2016). EGFR regulation of autophagy also impacts glial maintenance and degeneration of the
307 nervous system (Lee & Sun, 2015). Our ChIP-Seq analysis places FOXO as an upstream
308 regulator of MAPK/EGFR pathway to control autophagy and tissue maintenance during aging.

309 Our analysis also revealed that FOXO targets chromatin organization and nucleosome
310 assembly processes. This finding suggests that FOXO may be involved in the maintenance of
311 chromatin structure. Recent studies have shown that FOXO recruits SWI/SNF chromatin
312 remodelers to specific target sites to regulate lifespan in *C. elegans* (Riedel et al., 2013). Changes
313 in chromatin structure and overall loss of heterochromatin has long been an indicative

314 measurement of aging (Larson & Yuan, 2012; Wood et al., 2010; Zhang et al., 2015). It is likely
315 that FOXO plays an important role in maintaining chromatin structure and preventing age-related
316 chromatin remodeling. Interestingly, we found that many core histone genes are targeted by
317 FOXO. The binding of FOXO to these histone genes dramatically increases at old ages. It has
318 been shown that the transcripts of histone genes increase during yeast replicative aging, but the
319 levels of core histone proteins (e.g., H3, H2A) dramatically decrease with age (Feser et al.,
320 2010). Overexpression of histones or mutation of histone information regulator (Hir) increase
321 lifespan. How histone genes is transcriptional regulated during aging is unclear. Our findings
322 suggest that FOXO might be one of the molecular mechanisms that contribute to altered histone
323 expression during normal aging.

324 In summary, using a genome-wide approach we identified dynamic FOXO binding
325 activity during *Drosophila* aging. Our findings further support the important role of FOXO in
326 age-related transcriptional alterations and the regulation of tissue homeostasis and cellular
327 maintenance pathways. Further investigation of the functional significance of the altered FOXO
328 binding with age will be important in understanding how FOXO regulates organismal
329 homeostasis and longevity.

330

331 **Experimental Procedures**

332 *Fly culture and stocks*

333 Flies were maintained at 25 °C with 12 hour light/dark cycle, 60% humidity on agar-
334 based diet with 0.8% cornmeal, 10% sugar, and 2.5% yeast. yw^R flies (Bai et al., 2013) were used
335 as wild-type for ChIP-Seq. w^{1118} (Bloomington #5905) was used as a control genotype for *foxo*

336 mutants in RNA-Seq analysis. Female flies were collected and sorted 1-2 days after eclosion. To
337 age flies, vials contained 25-30 flies were transferred to fresh food every three days.

338 *CRISPR/Cas9 mutagenesis*

339 The *foxo* deletion lines were generated through CRISPR/Cas9 mutagenesis as previously
340 described (Ma et al., 2018). Briefly, two sgRNA plasmids targeting FOXO DNA binding domain
341 were injected into fly embryo. To genotyping G0 flies, single fly was homogenized in 50 μ l
342 squashing buffer (10 mM Tris buffer (pH 8.5), 25 mM NaCl, 1 mM EDTA, 200 μ g/ml
343 Proteinase K), incubated at 37 $^{\circ}$ C for 30 minutes, then followed by inactivation at 95 $^{\circ}$ C for 10
344 minutes. Screen primers for *foxo* deletion mutants were: F 5'-GGGGCAGATCCCCGCCAGC-
345 3', R 5'-GGGCGATTCTGAATAGCAGTGC-3'. The virgin females carrying the deletion were
346 backcrossed into *w¹¹¹⁸* male flies for five consecutive generations to mitigate background effects.

347 *Transcriptomic analysis (RNA-Seq)*

348 For transcriptomic analysis on the head tissues of aged flies and *foxo* deletion lines
349 (*foxo^{c431}*), forty heads from female flies were dissected and homogenized in a 1.5 ml tube
350 containing 1 ml of Trizol Reagent (Thermo Fisher Scientific, Waltham, MA, USA. Catalog
351 number: 15596026). Three biological replicates were performed for each age and genotype.
352 Total RNA was extracted following manufacturer instruction. TURBO DNA-free kit was used to
353 remove genomic DNA contamination (Thermo Fisher Scientific, Waltham, MA, USA. Catalog
354 number: AM1907). About 1 μ g of total RNA was used for sequencing library preparation.
355 PolyA-tailed RNAs were enriched by NEBNext Poly(A) mRNA Magnetic Isolation Module
356 (New England Biolabs (NEB), Ipswich, MA, USA. Catalog number: E7490S). RNA-Seq library
357 was prepared using NEBNext Ultra RNA library Prep Kit for Illumina (NEB, Ipswich, MA,
358 USA. Catalog number: E7420S). The libraries were pooled together in equimolar amounts to a

359 final 2 nM concentration. The normalized libraries were denatured with 0.1 M NaOH (Sigma)
360 and sequenced on the Illumina Miseq or Hiseq 2500 platforms (Single-end, Read length: 100
361 base pairs) (Illumina, San Diego, CA, USA).

362 *Chromatin immunoprecipitation sequencing (ChIP-Seq)*

363 Chromatin immunoprecipitation (ChIP) protocol was performed and modified from (Bai
364 et al., 2013). Two biological replicates were collected for each age and genotype. About 200
365 female flies were first anesthetized with FlyNap (Carolina Biological, Burlington, NC, USA.
366 Catalog number: 173010) and ground into a powder in liquid nitrogen. Crosslinking was
367 performed using 1% paraformaldehyde for 20 minutes followed by glycine quenching. The fly
368 homogenate was washed several times with 1X PBS supplemented with protease inhibitors, and
369 incubated briefly with cold cell lysis buffer (5 mM HEPES pH 7.6, 100 mM NaCl, 1 mM EDTA,
370 0.5% NP-40). Chromatin was extracted with nuclear lysis buffer (50 mM HEPES pH 7.6, 10 mM
371 EDTA, 0.1% Na-deoxycholate, 0.5% N-lauroylsarcosine), and sheared using Branson digital
372 sonifier 250, using 30%, with 30 seconds on, 30 seconds off for 5 cycles. Chromatin
373 immunoprecipitation was carried out using Protein G SureBeads (Bio-Rad, Hercules, CA, USA.
374 Catalog number: 1614023). Pre-cleaned chromatin extracts were incubated with anti-FOXO
375 antibody (Bai et al., 2013) and Protein G SureBeads to precipitate FOXO-DNA complexes.

376 DNA size selection and library prep were done using NEBNext Ultra II DNA library prep
377 kit and indexed using NEBNext multiplex oligos for Illumina (Primer set 1) (NEB, Ipswich, MA,
378 USA. Catalog number: E7645S, E7335S). DNA from either ChIP or input samples was mixed
379 with AMPure XP beads (Beckman Coulter Inc., Brea, CA, USA. Catalog number: A63881) to
380 select for a final library size of 320 bp. Samples were diluted to a final concentration of 2 nM for

381 Illumina sequencing on Illumina HiSeq 3000 (Single-end, Read length: 50 base pairs) (Illumina,
382 San Diego, CA, USA).

383 *Data processing of RNA-Seq and ChIP-Seq*

384 RNA-Seq reads were first mapped to the reference genome Dm6 with STAR_2.5.3a by
385 default parameter. The read counts for each gene were calculated by HTSeq-0.5.4e. The count
386 files were used as inputs to R package DESeq for normalization. The differential expression
387 genes were computed based on normalized counts from three biological replicates
388 ($|\log_2\text{foldchange}| > 1$, $\text{adj } p < 0.01$).

389 For ChIP-Seq, raw FASTQ reads were merged using mergePeaks (Homer suite) then
390 uploaded into Galaxy (usegalaxy.org) and checked for quality using FastQC. Files were then run
391 through FASTQ Groomer (<https://usegalaxy.org/u/dan/p/fastq>) for readability control before
392 mapping reads using Bowtie2 for single-end reads. *D. melanogaster* BDGP Release 6/dm6 was
393 used as the reference genome. BAM output files were converted to SAM using BAM-to-SAM
394 (<http://www.htslib.org/doc/samtools.html>) and sorted to generate peak images. Peak calling was
395 performed using MACS2. MACS2 FDR (q-value) was set for a peak detection cutoff of 0.05 and
396 did not build the shifting model. The MFOLD for the model was set from 10-50 to detect fold-
397 enrichment. Peak-calling was set to identify peaks 300 bp in length, and no peaks could exceed
398 10 Kb in size. After MACS2 peak identification, peak regions were expanded 2 kb (1 kb
399 upstream and 1 kb downstream) and assigned to nearby and overlapping genes using
400 BEDTools/intersect (<https://bedtools.readthedocs.io/en/latest/content/bedtools-suite.html>) with
401 Dm6.16 genome annotation file (UCSC, Santa Cruz, CA, USA). All non-protein coding
402 identified targets were removed from the data set manually based on annotation symbol.

403 *Venn Diagrams*

404 Venn diagram were created using the Bioinformatics and Evolutionary Genomics Venn
405 calculator at Ugent (<http://bioinformatics.psb.ugent.be/webtools/Venn/>). For cross species
406 comparisons, gene ID's were converted to fly ID's using DIOPT (<http://www.flyrnai.org/diopt>).
407 Genes that were the best possible match for each ortholog were selected for gene list comparison.

408 *Quantitative PCR (qPCR)*

409 Quantitative PCR was run on QuantStudio 3 (ThermoFisher Scientific, Waltham, MA
410 USA) with above ChIP and input library samples. PCR reaction was conducted using PowerUp
411 SYBR Green Master Mix (Life Technologies, CA, USA. Catalog number: 4402953). FOXO
412 binding enrichment was determined based on the fold-change between ChIP samples vs. Input
413 samples. The FOXO binding to Actin5C locus was used as a negative control. Two biological
414 and two technical replicates were performed for each age. Primers are listed in Table S2.

415 *Pathway and gene ontology analysis*

416 Pathway and gene ontology analysis was conducted using Panther
417 (<http://www.pantherdb.org/>), String (<https://string-db.org/>) and DAVID
418 (<https://david.ncifcrf.gov/>). All three methods were used to obtain a more complete picture of
419 shared regulation between datasets. KEGG pathway maps were obtained through KEGG
420 Pathway (<http://www.kegg.jp/kegg/pathway.html>).

421 *Motif analysis*

422 Motif analysis was conducted using Homer's *findMotifsGenome* script
423 (<http://homer.ucsd.edu/homer/ngs/peakMotifs.html>) to compare peak regions with Dm6.01
424 FASTA data from UCSC.

425 *List of raw datasets used*

426 ChIP-Seq datasets: GSE62580 (*Drosophila* aging fat body), GSE81100 (*Drosophila*
427 aging head tissue), GSE44686 (*Drosophila chico* heterozygotes FOXO ChIP), GSE15567
428 (Encode *C. elegans Daf-16* ChIP)

429 *Immunofluorescent staining*

430 Flies were anesthetized with FlyNap and dissected in 1X PBS. Fly tissues (muscle or fat
431 body) were then fixed in 4% paraformaldehyde for 20 minutes at room temperature. Tissue was
432 washed in 1X PBST (0.1% Triton X) and blocked with 5% normal goat serum (NGS) for 1 hour
433 at room temperature. Fly tissues were stained with anti-FOXO antibody in 1X PBST at a dilution
434 of 1:1000 for 16 hours at 4 °C on a rotator. Tissues were placed in secondary anti-body goat-anti-
435 rabbit conjugate Alexa Fluor 488 (Jackson ImmunoResearch Laboratories Inc., West Grove, PA,
436 USA) at a Dilution of 1:250 and kept in the dark at room temperature for 2 hours. The nucleus
437 was stained using SlowFade with DAPI. Images were captured using an epifluorescence-
438 equipped BX51WI microscope (Olympus, Waltham, MA, USA). Image deconvolution was
439 conducted using CellSens software (Olympus, Waltham, MA, USA), and compiled using ImageJ
440 Fiji.

441 *Statistical analysis*

442 GraphPad Prism (GraphPad Software, La Jolla, CA, USA) was used for statistical
443 analysis and to generate Boxplot. To compare the mean value of treatment groups versus that of
444 control, either student t-test or one-way ANOVA was performed using Dunnett's test for
445 multiple comparison.

446

447

448

449 **Acknowledgments**

450 We thank Bloomington Drosophila Stock Center for fly stocks. We thank Michael Baker and
451 DNA Facility at Iowa State University (ISU) for help with RNA-Seq analysis, Usha Muppirla
452 and Andrew Severin from ISU Genome Informatics Facility (GIF) for assistance with
453 bioinformatics. We thank Christian Riedel for providing *C. elegans Daf-16* ChIP-Seq data. This
454 work was supported by NIH/NIA R00 AG048016 to HB, AFAR Research Grants for Junior
455 Faculty to HB, and National Program on Key Basic Research Project of China
456 2016YFA0501900 to NL.

457 **Author's Contributions Statement**

458 Conceived and designed the experiments: AB XW NL HB. Performed the experiments: AB XW.
459 Analyzed the data: AB XW MT NL HB. Wrote the paper: AB XW NL HB. All authors reviewed
460 and approved the manuscript.

461 **Availability of data and materials**

462 The raw data files of sequencing experiments have been deposited in the NCBI Gene Expression
463 Omnibus. The accession number for RNA-Seq data is GSE122470
464 (<https://www.ncbi.nlm.nih.gov/geo/query/acc.cgi?acc=GSE122470>).
465 The accession number for ChIP-Seq data is GSE121102
466 (<https://www.ncbi.nlm.nih.gov/geo/query/acc.cgi?acc=GSE121102>).

467 **Competing Interests**

468 The authors declare that no competing interest exists.

469

470

471

472 **Figure Legends**

473

474 **Figure 1. FOXO exhibits constitutive nuclear localization in young and old adult fat body.**

475 **A)** Abdominal fat body of wild-type flies (yw^R) stained with anti-FOXO at young (2 weeks) and
476 old ages (5 weeks). **B)** Quantification of Pearson correlation coefficient (R) between FOXO and
477 DAPI staining in fat body tissue. **C)** FOXO immunostaining in young and old indirect flight
478 muscles of wild-type flies (yw^R). **D)** Quantification of Pearson correlation coefficient (R)
479 between FOXO and DAPI in indirect flight muscles. Scale bar: 20 μm . Student *t*-test (***, $p <$
480 0.001; ns: not significant).

481

482 **Figure 2. FOXO binding activity decreases with age. A)** The number of genes targeted by

483 FOXO at young (2 weeks) and old ages (5 weeks). **B)** Age-dependent FOXO binding at *jim*

484 locus. **C)** Age-dependent FOXO binding at *his1:CG33804* and *his2B:CG33908* loci. **D)** GO

485 terms for FOXO-targeted pathways uniquely enriched in young or old flies. **E)** qPCR validation

486 of the FOXO binding enrichment at the selected FOXO targeted genomic loci. FOXO binding at

487 Act5C locus serves as an internal control. The enrichment value is calculated as the fold-change

488 (f. c.) of the FOXO binding (ChIP vs. Input) between FOXO-targeted loci and Act5C locus.

489 Student *t*-test (***, $p < 0.001$; **, $p < 0.01$; *, $p < 0.05$).

490

491 **Figure 3. FOXO target genes show age-dependent transcriptional changes. A)** The number

492 of FOXO-bound genes that are differentially expressed in aging fat body. **B)** Representative

493 biological processes enriched for age-regulated FOXO targets in fat body. **C)** The number of

494 FOXO-bound genes that are differentially expressed in aging head tissue. **D)** Representative
495 biological processes enriched for age-regulated FOXO targets in adult head tissue.

496

497 **Figure 4. The altered of FOXO binding correlates with age-related transcriptional changes**

498 **of FOXO targets. A)** The diagram showing *foxo* locus and the target sites of the guiding RNAs

499 (highlighted in red) used to generate *foxo*^{c431} loss-of-function mutants by CRISPR/Cas9

500 mutagenesis. PAM: Protospacer adjacent motifs (highlighted in blue). **B)** Western blots to verify

501 the expression of FOXO proteins in *foxo*^{c431} loss-of-function mutants. β -actin as a loading

502 control. **C)** The number of FOXO target genes that are differentially expressed between *foxo*^{c431}

503 mutants and wild-type flies. **D)** Age-dependent transcriptional changes of FOXO target genes.

504 Boxplots represent the mean fold change of genes at Day 15 (d15), Day 30 (d30) and Day 45

505 (d45), relative to that of Day 3 (d3) in aging head tissue (Student *t*-test).

506 **Figure 5. FOXO binding differs between wild-type and insulin/IGF mutants. A)**

507 Comparison of FOXO target genes between wild-type and *chico* mutants. **B)** Overlap between

508 age-dependent differentially expressed genes (fat body and head) and FOXO-bound targets

509 (wild-type and *chico* mutants). **C)** GO terms uniquely enriched in wild-type or *chico* mutants. **D)**

510 Daf-16-bound targets genes in wild-type *C. elegans* and *Daf-2* mutants. **E)** Shared pathways

511 targeted by both fly FOXO and worm Daf-16 in wild-type animals. Enriched *C. elegans* GO

512 terms are shown.

513

514 **Table 1:**

515 Lists of motifs that are enriched among FOXO target sites in wild-type flies.

516

517 **Supporting information:**

518 **Figure S1.** Abdominal fat body and flight muscle of wild-type flies (*Ore^R*) stained with anti-
519 FOXO at young (2 weeks) and old age (5 weeks). Scale bar: 20 μ m.

520 **Figure S2. A)** The total number of raw reads and Bowtie alignment percentage for individual
521 ChIP-Seq sample. **B)** Plot correlation matrix showing the overall correlation among young and
522 old ChIP and input samples.

523 **Figure S3.** FOXO target genes in Hippo signaling pathway. Unique FOXO targets in wild-type
524 flies (*yw^R*) are highlighted in blue. Unique FOXO targets in *chico* mutants are highlighted in
525 orange. Shared targets are highlighted in green.

526 **Figure S4.** FOXO target genes in MAPK/EGFR signaling pathway. Unique FOXO targets in
527 wild-type flies (*yw^R*) are highlighted in blue. Unique FOXO targets in *chico* mutants are
528 highlighted in orange. Shared targets are highlighted in green.

529 **Table S1:**

530 Lists of peaks, target genes, and GO terms

531 **Table S2:**

532 Lists of primers used in qPCR analysis

533

534 **References:**

- 535 Alic, N., Andrews, T. D., Giannakou, M. E., Papatheodorou, I., Slack, C., Hoddinott, M. P., . . . Partridge, L.
536 (2011). Genome-wide dFOXO targets and topology of the transcriptomic response to stress and
537 insulin signalling. *Mol Syst Biol*, 7, 502. doi: 10.1038/msb.2011.36
- 538 Armoni, M., Harel, C., Karni, S., Chen, H., Bar-Yoseph, F., Ver, M. R., . . . Karnieli, E. (2006). FOXO1
539 represses peroxisome proliferator-activated receptor-gamma1 and -gamma2 gene promoters in
540 primary adipocytes. A novel paradigm to increase insulin sensitivity. *J Biol Chem*, 281(29),
541 19881-19891. doi: 10.1074/jbc.M600320200
- 542 Bai, H., Kang, P., Hernandez, A. M., & Tatar, M. (2013). Activin signaling targeted by insulin/dFOXO
543 regulates aging and muscle proteostasis in *Drosophila*. *PLoS Genet*, 9(11), e1003941. doi:
544 10.1371/journal.pgen.1003941

- 545 Brunet, A., Bonni, A., Zigmond, M. J., Lin, M. Z., Juo, P., Hu, L. S., . . . Greenberg, M. E. (1999). Akt
546 promotes cell survival by phosphorylating and inhibiting a Forkhead transcription factor. *Cell*,
547 *96*(6), 857-868.
- 548 Daitoku, H., Sakamaki, J., & Fukamizu, A. (2011). Regulation of FoxO transcription factors by acetylation
549 and protein-protein interactions. *Biochim Biophys Acta*, *1813*(11), 1954-1960. doi:
550 10.1016/j.bbamcr.2011.03.001
- 551 Dansen, T. B., & Burgering, B. M. (2008). Unravelling the tumor-suppressive functions of FOXO proteins.
552 *Trends Cell Biol*, *18*(9), 421-429. doi: 10.1016/j.tcb.2008.07.004
- 553 Demontis, F., & Perrimon, N. (2010). FOXO/4E-BP signaling in Drosophila muscles regulates organism-
554 wide proteostasis during aging. *Cell*, *143*(5), 813-825. doi: 10.1016/j.cell.2010.10.007
- 555 Eijkelenboom, A., Mokry, M., Smits, L. M., Nieuwenhuis, E. E., & Burgering, B. M. (2013). FOXO3
556 selectively amplifies enhancer activity to establish target gene regulation. *Cell Rep*, *5*(6), 1664-
557 1678. doi: 10.1016/j.celrep.2013.11.031
- 558 Essers, M. A., Weijzen, S., de Vries-Smits, A. M., Saarloos, I., de Ruiter, N. D., Bos, J. L., & Burgering, B. M.
559 (2004). FOXO transcription factor activation by oxidative stress mediated by the small GTPase
560 Ral and JNK. *EMBO J*, *23*(24), 4802-4812. doi: 10.1038/sj.emboj.7600476
- 561 Feser, J., Truong, D., Das, C., Carson, J. J., Kieft, J., Harkness, T., & Tyler, J. K. (2010). Elevated histone
562 expression promotes life span extension. *Mol Cell*, *39*(5), 724-735. doi:
563 10.1016/j.molcel.2010.08.015
- 564 Furuyama, T., Nakazawa, T., Nakano, I., & Mori, N. (2000). Identification of the differential distribution
565 patterns of mRNAs and consensus binding sequences for mouse DAF-16 homologues.
566 *Biochemical Journal*, *349*, 629-634. doi: Doi 10.1042/0264-6021:3490629
- 567 Greer, E. L., & Brunet, A. (2005). FOXO transcription factors at the interface between longevity and
568 tumor suppression. *Oncogene*, *24*(50), 7410-7425. doi: 10.1038/sj.onc.1209086
- 569 Hazan, R. B., & Norton, L. (1998). The epidermal growth factor receptor modulates the interaction of E-
570 cadherin with the actin cytoskeleton. *J Biol Chem*, *273*(15), 9078-9084.
- 571 Heallen, T., Morikawa, Y., Leach, J., Tao, G., Willerson, J. T., Johnson, R. L., & Martin, J. F. (2013). Hippo
572 signaling impedes adult heart regeneration. *Development*, *140*(23), 4683-4690. doi:
573 10.1242/dev.102798
- 574 Holzenberger, M., Dupont, J., Ducos, B., Leneuve, P., Geloën, A., Even, P. C., . . . Le Bouc, Y. (2003). IGF-1
575 receptor regulates lifespan and resistance to oxidative stress in mice. *Nature*, *421*(6919), 182-
576 187. doi: 10.1038/nature01298
- 577 Huang, H., & Tindall, D. J. (2006). FOXO factors: a matter of life and death. *Future Oncol*, *2*(1), 83-89. doi:
578 10.2217/14796694.2.1.83
- 579 Jiang, H., Grenley, M. O., Bravo, M. J., Blumhagen, R. Z., & Edgar, B. A. (2011). EGFR/Ras/MAPK signaling
580 mediates adult midgut epithelial homeostasis and regeneration in Drosophila. *Cell Stem Cell*,
581 *8*(1), 84-95. doi: 10.1016/j.stem.2010.11.026
- 582 Kenyon, C., Chang, J., Gensch, E., Rudner, A., & Tabtiang, R. (1993). A *C. elegans* mutant that lives twice
583 as long as wild type. *Nature*, *366*(6454), 461-464. doi: 10.1038/366461a0
- 584 Kitamura, T., Nakae, J., Kitamura, Y., Kido, Y., Biggs, W. H., 3rd, Wright, C. V., . . . Accili, D. (2002). The
585 forkhead transcription factor Foxo1 links insulin signaling to Pdx1 regulation of pancreatic beta
586 cell growth. *J Clin Invest*, *110*(12), 1839-1847. doi: 10.1172/JCI16857
- 587 Kops, G. J., Dansen, T. B., Polderman, P. E., Saarloos, I., Wirtz, K. W., Coffey, P. J., . . . Burgering, B. M.
588 (2002). Forkhead transcription factor FOXO3a protects quiescent cells from oxidative stress.
589 *Nature*, *419*(6904), 316-321. doi: 10.1038/nature01036
- 590 Larson, J. L., & Yuan, G. C. (2012). Chromatin states accurately classify cell differentiation stages. *PLoS*
591 *One*, *7*(2), e31414. doi: 10.1371/journal.pone.0031414

- 592 Lee, Y. M., & Sun, Y. H. (2015). Maintenance of glia in the optic lamina is mediated by EGFR signaling by
593 photoreceptors in adult *Drosophila*. *PLoS Genet*, *11*(4), e1005187. doi:
594 10.1371/journal.pgen.1005187
- 595 Lehtinen, M. K., Yuan, Z., Boag, P. R., Yang, Y., Villen, J., Becker, E. B., . . . Bonni, A. (2006). A conserved
596 MST-FOXO signaling pathway mediates oxidative-stress responses and extends life span. *Cell*,
597 *125*(5), 987-1001. doi: 10.1016/j.cell.2006.03.046
- 598 Lopez-Otin, C., Blasco, M. A., Partridge, L., Serrano, M., & Kroemer, G. (2013). The hallmarks of aging.
599 *Cell*, *153*(6), 1194-1217. doi: 10.1016/j.cell.2013.05.039
- 600 Ma, Z., Wang, H., Cai, Y., Wang, H., Niu, K., Wu, X., . . . Liu, N. (2018). Epigenetic drift of H3K27me3 in
601 aging links glycolysis to healthy longevity in *Drosophila*. *Elife*, *7*. doi: 10.7554/eLife.35368
- 602 Mao, B., Gao, Y., Bai, Y., & Yuan, Z. (2015). Hippo signaling in stress response and homeostasis
603 maintenance. *Acta Biochim Biophys Sin (Shanghai)*, *47*(1), 2-9. doi: 10.1093/abbs/gmu109
- 604 Martins, R., Lithgow, G. J., & Link, W. (2016). Long live FOXO: unraveling the role of FOXO proteins in
605 aging and longevity. *Aging Cell*, *15*(2), 196-207. doi: 10.1111/acer.12427
- 606 Medema, R. H., Kops, G. J., Bos, J. L., & Burgering, B. M. (2000). AFX-like Forkhead transcription factors
607 mediate cell-cycle regulation by Ras and PKB through p27kip1. *Nature*, *404*(6779), 782-787. doi:
608 10.1038/35008115
- 609 Murphy, L. J. (2006). Insulin-like growth factor-I: a treatment for type 2 diabetes revisited.
610 *Endocrinology*, *147*(6), 2616-2618. doi: 10.1210/en.2006-0343
- 611 Olmos, Y., Valle, I., Borniquel, S., Tierrez, A., Soria, E., Lamas, S., & Monsalve, M. (2009). Mutual
612 dependence of Foxo3a and PGC-1alpha in the induction of oxidative stress genes. *J Biol Chem*,
613 *284*(21), 14476-14484. doi: 10.1074/jbc.M807397200
- 614 Polvani, S., Tarocchi, M., & Galli, A. (2012). PPARgamma and Oxidative Stress: Con(beta) Catenating
615 NRF2 and FOXO. *PPAR Res*, *2012*, 641087. doi: 10.1155/2012/641087
- 616 Rera, M., Clark, R. I., & Walker, D. W. (2012). Intestinal barrier dysfunction links metabolic and
617 inflammatory markers of aging to death in *Drosophila*. *Proc Natl Acad Sci U S A*, *109*(52), 21528-
618 21533. doi: 10.1073/pnas.1215849110
- 619 Riedel, C. G., Downen, R. H., Lourenco, G. F., Kirienko, N. V., Heimbucher, T., West, J. A., . . . Ruvkun, G.
620 (2013). DAF-16 employs the chromatin remodeller SWI/SNF to promote stress resistance and
621 longevity. *Nat Cell Biol*, *15*(5), 491-501. doi: 10.1038/ncb2720
- 622 Slack, C., Giannakou, M. E., Foley, A., Goss, M., & Partridge, L. (2011). dFOXO-independent effects of
623 reduced insulin-like signaling in *Drosophila*. *Aging Cell*, *10*(5), 735-748. doi: 10.1111/j.1474-
624 9726.2011.00707.x
- 625 Tan, X., Lambert, P. F., Rapraeger, A. C., & Anderson, R. A. (2016). Stress-Induced EGFR Trafficking:
626 Mechanisms, Functions, and Therapeutic Implications. *Trends Cell Biol*, *26*(5), 352-366. doi:
627 10.1016/j.tcb.2015.12.006
- 628 Tatar, M., Kopelman, A., Epstein, D., Tu, M. P., Yin, C. M., & Garofalo, R. S. (2001). A mutant *Drosophila*
629 insulin receptor homolog that extends life-span and impairs neuroendocrine function. *Science*,
630 *292*(5514), 107-110. doi: 10.1126/science.1057987
- 631 Udan, R. S., Kango-Singh, M., Nolo, R., Tao, C., & Halder, G. (2003). Hippo promotes proliferation arrest
632 and apoptosis in the Salvador/Warts pathway. *Nat Cell Biol*, *5*(10), 914-920. doi:
633 10.1038/ncb1050
- 634 van der Horst, A., & Burgering, B. M. (2007). Stressing the role of FoxO proteins in lifespan and disease.
635 *Nat Rev Mol Cell Biol*, *8*(6), 440-450. doi: 10.1038/nrm2190
- 636 van der Vos, K. E., & Coffey, P. J. (2008). FOXO-binding partners: it takes two to tango. *Oncogene*, *27*(16),
637 2289-2299. doi: 10.1038/onc.2008.22
- 638 Webb, A. E., Kundaje, A., & Brunet, A. (2016). Characterization of the direct targets of FOXO
639 transcription factors throughout evolution. *Aging Cell*, *15*(4), 673-685. doi: 10.1111/acer.12479

- 640 Webb, A. E., Pollina, E. A., Vierbuchen, T., Urban, N., Ucar, D., Leeman, D. S., . . . Brunet, A. (2013).
641 FOXO3 shares common targets with ASCL1 genome-wide and inhibits ASCL1-dependent
642 neurogenesis. *Cell Rep*, 4(3), 477-491. doi: 10.1016/j.celrep.2013.06.035
- 643 Wood, J. G., Hillenmeyer, S., Lawrence, C., Chang, C., Hosier, S., Lightfoot, W., . . . Helfand, S. L. (2010).
644 Chromatin remodeling in the aging genome of *Drosophila*. *Aging Cell*, 9(6), 971-978. doi:
645 10.1111/j.1474-9726.2010.00624.x
- 646 Yamamoto, R., & Tatar, M. (2011). Insulin receptor substrate chico acts with the transcription factor
647 FOXO to extend *Drosophila* lifespan. *Aging Cell*, 10(4), 729-732. doi: 10.1111/j.1474-
648 9726.2011.00716.x
- 649 Zhang, W., Li, J., Suzuki, K., Qu, J., Wang, P., Zhou, J., . . . Belmonte, J. C. (2015). Aging stem cells. A
650 Werner syndrome stem cell model unveils heterochromatin alterations as a driver of human
651 aging. *Science*, 348(6239), 1160-1163. doi: 10.1126/science.aaa1356
- 652 Zhong, M., Niu, W., Lu, Z. J., Sarov, M., Murray, J. I., Janette, J., . . . Snyder, M. (2010). Genome-wide
653 identification of binding sites defines distinct functions for *Caenorhabditis elegans* PHA-4/FOXA
654 in development and environmental response. *PLoS Genet*, 6(2), e1000848. doi:
655 10.1371/journal.pgen.1000848
- 656

Figure 1

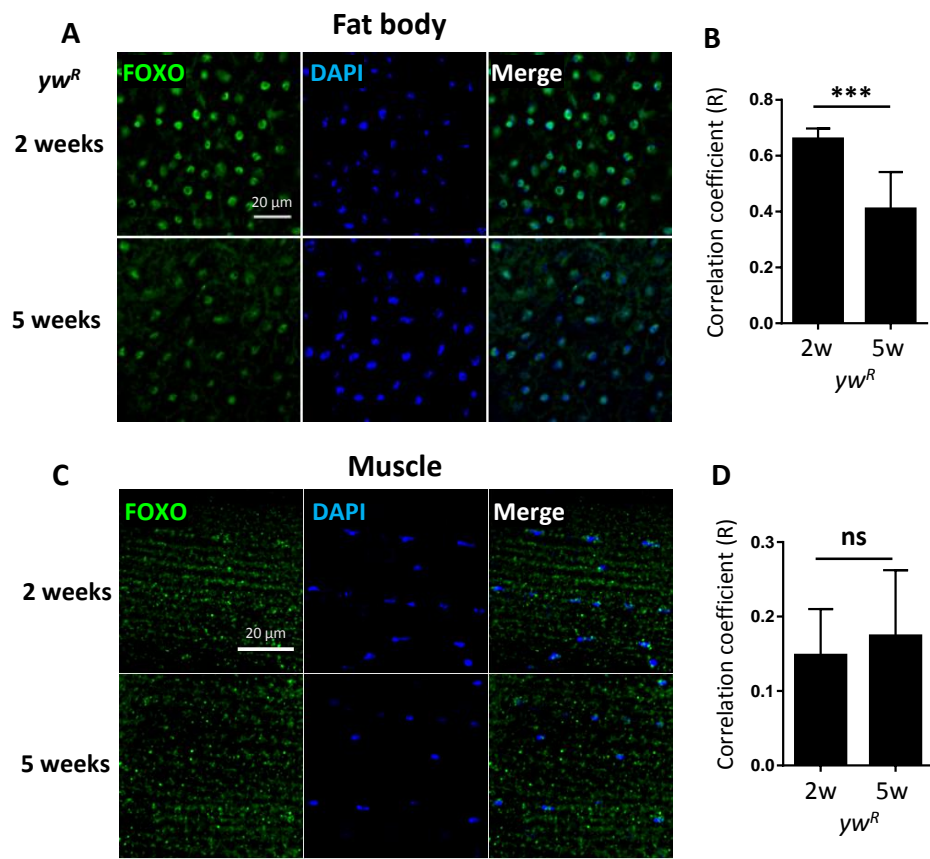


Figure 2

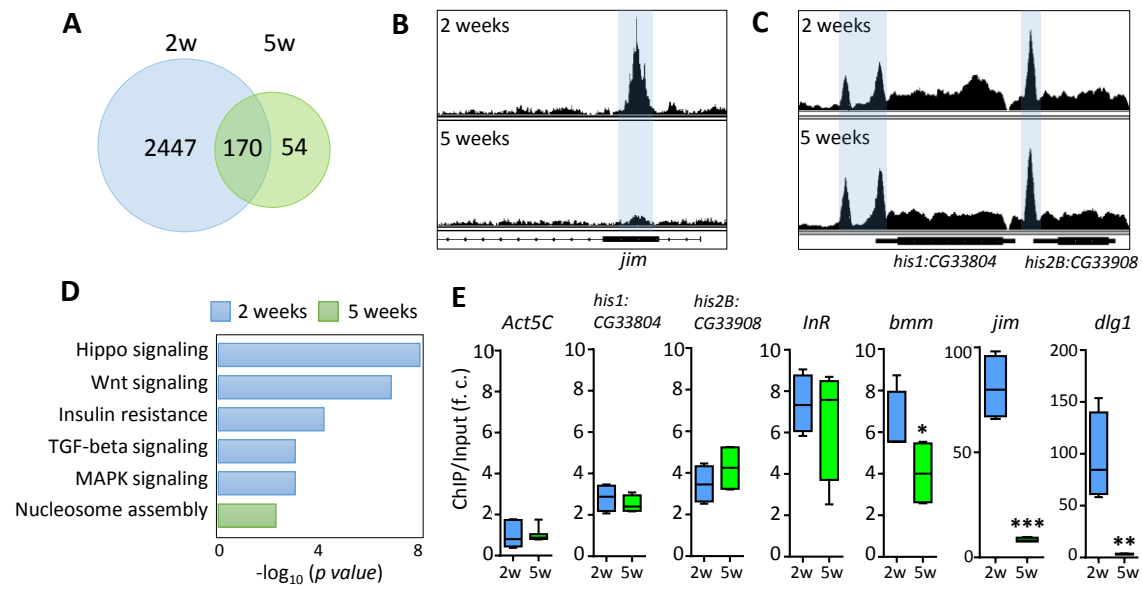


Figure 3

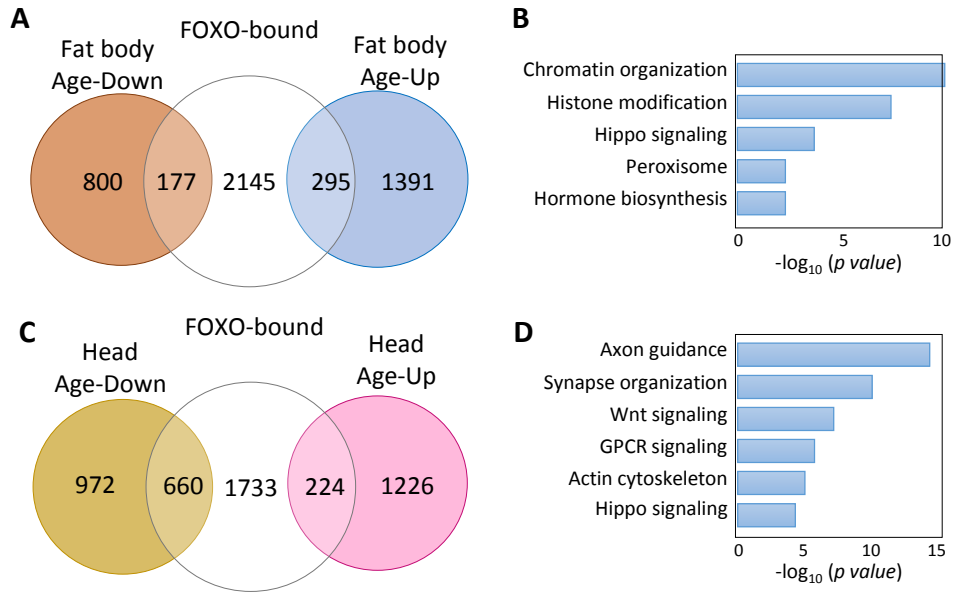


Figure 5

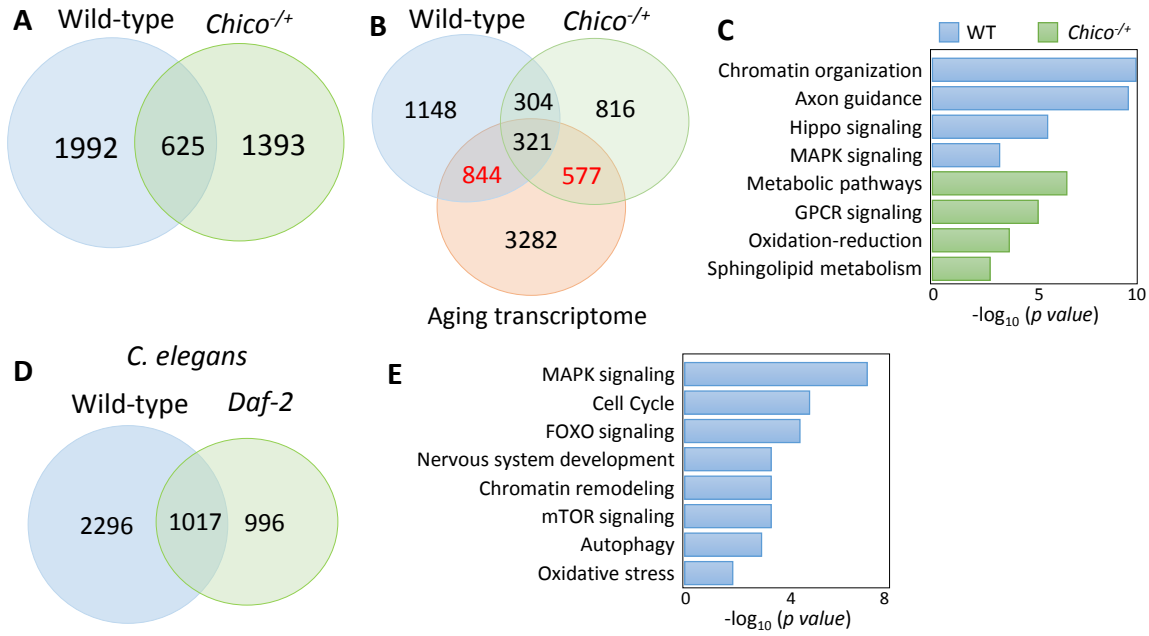


Table 1







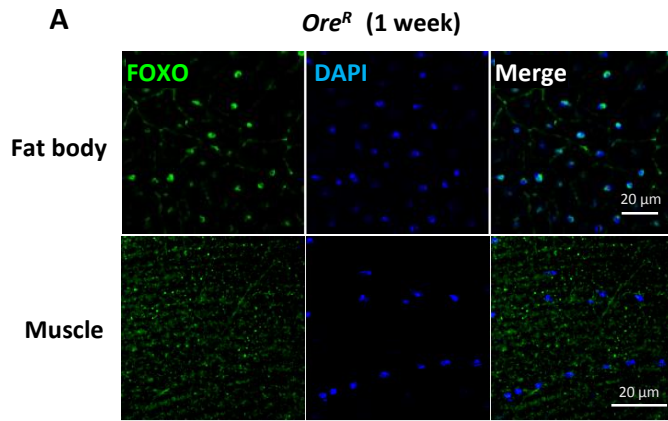
motif	P-value	# targets with motif	predicted to be bound by
Enriched known binding motifs compared to whole genome			
	1.00E-70	842	Trl(Zf)/S2-GAGAFactor
motif			
P-value			
% targets with motif			
predicted to be bound by			
Enriched de novo binding motifs compared to whole genome			
	1.00E-164	47.58%	RAP1/MA0359.1/Jaspar(0.703)
	1.00E-130	44.94%	hb/dmmpmm(Noyes)/fly(0.726)
	1.00E-82	35.48%	Adf1/dmmpmm(Bergman)/fly(0.664)
	1.00E-56	27.59%	Aef1/dmmpmm(Pollard)/fly(0.851)
motif			
P-value			
# targets with motif			
predicted to be bound by			
Enriched known binding motifs all organisms			
	1.00E-04	1012	Foxo1(Forkhead)/RAW-Foxo1-ChIP-Seq(Fan_et_al.)/Homer

Figure S1



A

Sample	Raw reads	% Alignment
2-week-old ChIP-1	25,554,421	85.74%
2-week-old input-1	40,459,444	96.09%
2-week-old ChIP-2	15,933,943	73.70%
2-week-old input-2	34,196,540	96.26%
5-week-old ChIP-1	15,880,701	92.00%
5-week-old input-1	73,535,040	95.06%
5-week-old ChIP-2	14,515,822	91.76%
5-week-old input-2	40,815,124	95.98%

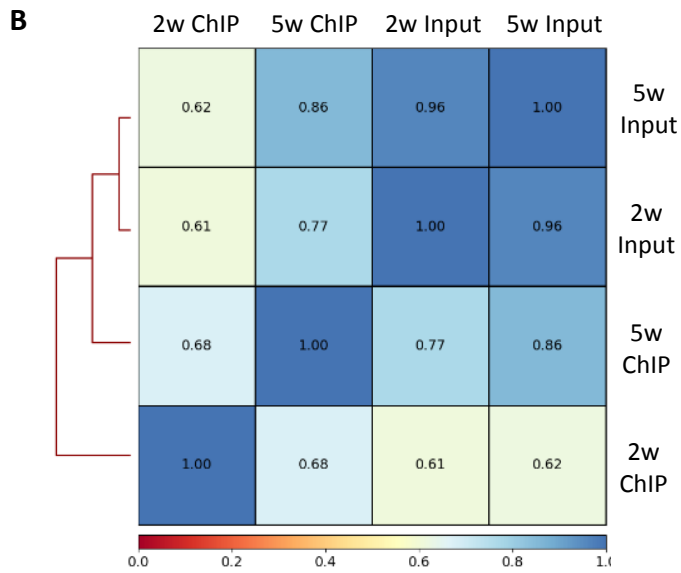


Figure S3

Drosophila Hippo Signaling Pathway

- Unique FOXO targets in wild-type
- Unique FOXO targets in *chico*^{+/+}
- Shared FOXO targets

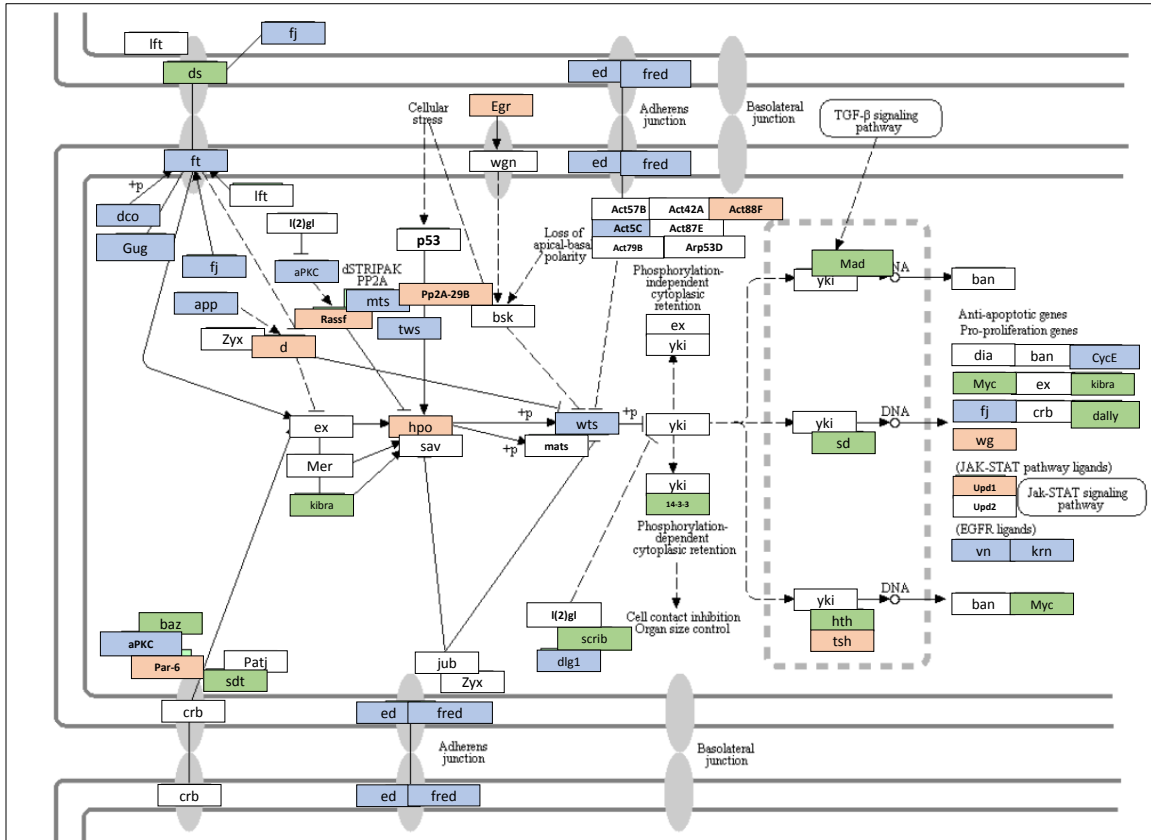


Figure S4

Drosophila MAPK/EGFR Signaling Pathway

- Unique FOXO targets in wild-type
- Unique FOXO targets in *chico*^{+/+}
- Shared FOXO targets

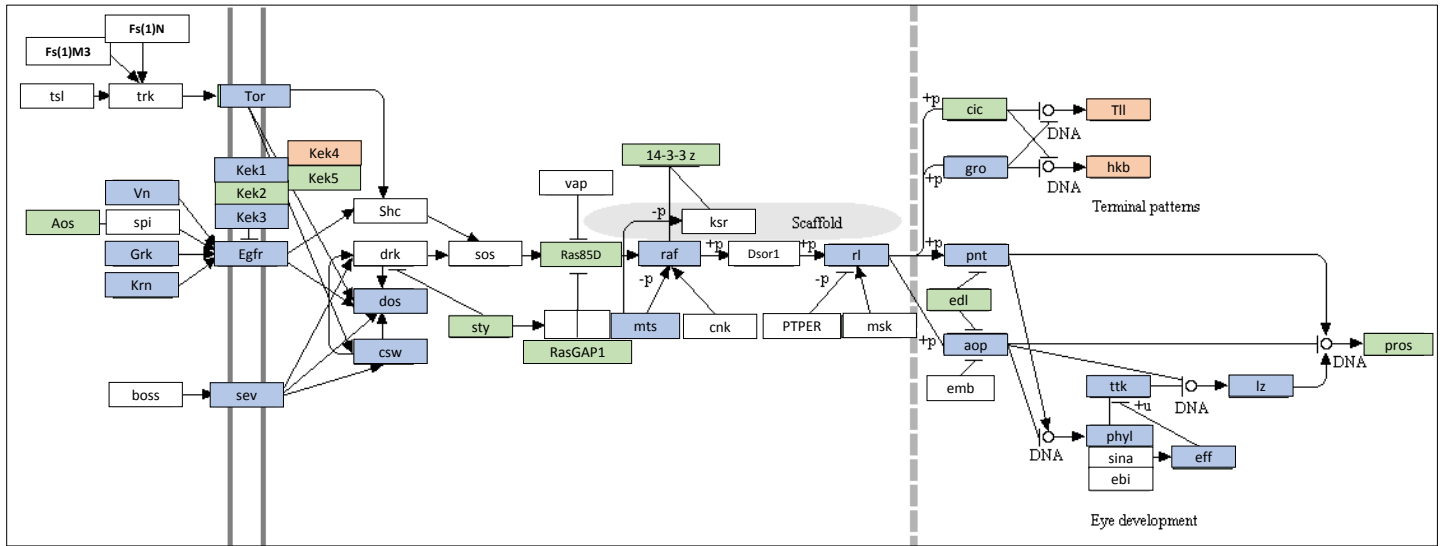


Table S2

Primer name	Direction	Sequence 5'->3'
<i>Act5C</i>	Forward	TCGCGATTTGACCGACTACCTGAT
	Reverse	TGATGTCACGGACGATTTACGCT
<i>his1:CG33804</i>	Forward	ACACTTCAAGCAAACCTTGACA
	Reverse	CCAACCTCCTTTGCTCTGAT
<i>his2B:CG33908</i>	Forward	TTCAGGGCTACAACGTTCC
	Reverse	AAACTGAATGCGACCAACATT
<i>InR</i>	Forward	ATAGAACGACGCACTTTCCC
	Reverse	CGCGCGCTCTCCTATTATTTA
<i>bmm</i>	Forward	CACCGCGCCGCAATGAATGTATAA
	Reverse	TTCAATCACTGTTTGTGGTCGGC
<i>jim</i>	Forward	GAGGCGGGTTTAAGGCTATT
	Reverse	CAGGCAAACAAATCAAAGCAAAC
<i>dlg1</i>	Forward	CTGTTCTCTGTTCTTCTTCTT
	Reverse	AGTAGTAGTAGTAGTGGTAGTAGTATAG